Journal of
Nanoscience and Nanotechnology
Vol. 12, 2489–2495, 2012

Analytical Modeling of the Ion Number Fluctuations in Biological Ion Channels

Santosh Pandey

Electrical and Computer Engineering, Coover Hall, Iowa State University, Ames, IA-50011, USA

Ion channels are transmembrane proteins that regulate and maintain the ionic concentrations across the cell membrane. Modeling the atomistic-level ionic flux through these channels is crucial for the understandingof several neurological diseases and related pharmaceutical discoveries. Experimental techniques now provide information about the channel's physical structure which helps in developing realisticion transport models. Ions entering a channel follow different trajectories as they traverse the channel; each associated with a certain probability. Quantities that explain these trajectories are the translocation and return probabilities, average lifetime, and spectral density (an experimentally accessible parameter) of ion number fluctuations. Theoretical analysis of ion transport has been limited to low-resolution continuum diffusion-based or kinetic-based models. Such analytical models fail to include key factors affecting the ionic conduction. In this paper, we extend previous models by an electro-diffusion model incorporating the effects of electric field, energy barrier, and rate-limited association/dissociation of ions with surface charges inside the channel. Survival probability and spectral density are derived from the analytical model.

Keywords: Molecular Dynamics, Ion Channel, Spectral Density, Green Function.

RESEARCH ARTICLE

1. INTRODUCTION

Ion channels are pores in a cell membrane that routinely allow the exchange of specific ions across them. These channels play a central role in regulating the chemical and electrostatic gradients across the cell membrane which guides the movement of ions in/out of the cell. The physics of ion movement through the ion channels (when open) is simple: electrodiffusion and convection. The challenge lies in predicting the transport of ions of different types and concentrations across ion channel structures that can have unique topographies. Additionally, channel proteins have a fixed charge that demands counter ions in a nearby ionic atmosphere. Imbalances in ion concentrations create strong electric fields, and the non-equilibrium behavior of ions in such fields is crucial for regulating the open/closed states of the channel. Recent experimental advances and new molecular-level simulation modelsare helping us understand the complex mechanisms involved in ion transport through channels.[1]

Till recently, theoretical analysis of ion transport has been limited to diffusion-induced transport of metabolites.[2] Even though diffusion remains to be the main transport mechanism, electric field-induced drift velocity adds to the momentum of the transporting ions. This transmembrane potential gradient, which drives ion channel gating and permeation, should be considered an integral player in any ion channel modeling analysis. Besides drift and diffusion, ions are also being randomly associated or dissociated with the charged surface proteins in the channel's vestibule. These surface charges are known to influence the gating, conductance, and toxin-binding effects of KcsA ion-channels, and their actual physical locations are presumed to be in the selectivity filter.[3] So, it is also important to include the effects of association/dissociation of the metabolites in any analytical model which affects the measured spectral density of ion number fluctuations in an ion channel.

An ion entering a channel can either return to the source reservoir or traverse the channel's vestibule and reach the sink reservoir successfully. Key quantities that describe the process would be the translocation and return probabilities, average translocation lifetime inside the channel and the spectral density of ion number fluctuations during the ion flow.[4] In this work, a physics-based model is presented that incorporates the effects of ion mobility, constant electric field, and association/dissociation of ions inside a cylindrical ion-channel. The main focus is on ion transport through a channel, including the interaction of an ion with surface protein charges but ignoring ion–ion interactions. In the next section, we derive a general expression of the probability density function (p.d.f.) related to the particle

number fluctuations inside an ion-channel. The p.d.f. is derived in the axial direction and incorporates rate constants related to the association/dissociation of ions. The generalized expression for the p.d.f. is represented in terms of Green function. In the following section, we derive the exact Green functions for diffusion-induced ion transport in the presence of a constant electric field. Using a transformation, we demonstrate a method of handling the effects of carrier mobility and electric field in such models based on Green functions. Lastly, we derive the exact expression of the p.d.f., survival probability, and spectral density of particle number fluctuations. The results are plotted using Maple™ and simulation plots are provided. Such models can be extended to describe other charge transport processes in nature (besides ion transport) such as charge migration along polymers or translocation of DNA chains through artificial nanopores.[5]

2. FORMULATION

Consider acylindrical ion channel of length L with two bulk reservoirs: source and sink (Fig. 1). The ions flow from source to sink guided by a concentration gradient and an electric field. We assume that the ions are very few in number inside the channel and mutually non-interacting. The ions can, however, interact with a single surface site inside the channel through association/dissociation. Let us denote by $p(x,t)$, the probability density of a free ion at an axial distance x along the channel and at a time t, whereas $q(x,t)$ denotes the probability density of finding an immobile ion bound temporarily with surface protein charges. These functions obey the following equations,[6–8]

$$\frac{\partial p(x,t)}{\partial t} = £p(x,t) - k_a\delta(x-a)p(x,t) + k_d\delta(x-a)q(x,t) \quad (1a)$$

$$\frac{\partial q(x,t)}{\partial t} = k_a\delta(x-a)p(x,t) - k_d\delta(x-a)q(x,t) \quad (1b)$$

where $x=a$ is the contact site of association/dissociation, k_a is the rate of association, and k_d is the rate of dissociation. In terms of the potential energy $U(x)$ and the diffusion constant D_P, diffusion operator £ in one-dimension is given as,[7]

$$£ = D_P\frac{\partial}{\partial x}e^{-U(x)}\frac{\partial}{\partial x}e^{U(x)} \quad (2)$$

To obtain solutions of the two functions, $p(x,t)$ and $q(x,t)$, we introduce the Green function $G(x,s\mid x_o)$ in the Laplace domain satisfying $(s-£)G(x,s\mid x_o)=\delta(x-a)$, with an initial impulse $Q_O\delta(x-x_O)$ of amplitude Q_O at an axial distance $x=x_o$. With this initial condition, we assume an ion impulse is externally applied precisely at $x=x_o$ and time progression of this impulse is analyzed to obtain the system impulse response. Furthermore, an absorbing boundary condition for both source and sink reservoirs is assumed. As shown in Appendix A, the generalized solutions of $p(x,t)$ and $q(x,t)$ in the Laplace domain can be written as:

$$\overline{p}(x,s\mid x_o) = \frac{G(a,s\mid x_o)}{1+(sk_a/(s+k_d))G(a,s\mid a)}\left(-\frac{sk_a}{s+k_d}\right)\times G(x,s\mid a)+G(x,s\mid x_o) \quad (3a)$$

$$\bar{q}(x,s\mid x_o) = \frac{G(a,s\mid x_o)}{1+(sk_a/(s+k_d))G(a,s\mid a)}\times\left(\frac{k_a}{s+k_d}\right)\delta(x-a) \quad (3b)$$

where $\overline{p}(x,s\mid x_o)$ and $\bar{q}(x,s\mid x_o)$ denote the Laplace transforms of $p(x,t)$ and $q(x,t)$ respectively with an initial impulse at $x=x_o$. Equations (3a) and (3b) describe the probability density functions (p.d.f.) corresponding to an ion in the unbound state or in the bound state. Next, we will derive the expression of the Green function $G(x,s\mid x_o)$ for substitution into Eq. (3a) to obtain the exact analytical expression forthe p.d.f. of a free ion, $\overline{p}(x,s\mid x_o)$. This result willthen be used to derive the spectral density of ion number fluctuations in the ion channel.

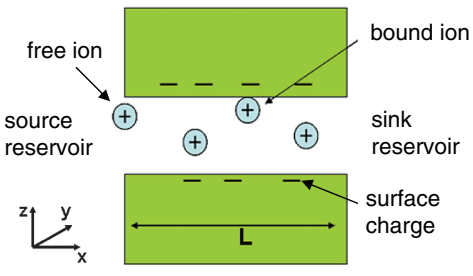

Fig. 1. A sketch of the cylindrical ion channel of length L and two reservoirs at either end. An ion traverses from the source to the sink reservoir. The free ions can occasionally bind reversibly with surface protein charges embedded in the channel's wall.

3. GREEN FUNCTIONS

We assume, for simplicity, one-dimensional transport of ions in a constant electric field ε. The current density and the continuity equations can be written as,[9]

$$J_P = q\mu_P\varepsilon g(x,t) - qD_P\partial g(x,t)/\partial x \quad (4a)$$

$$\partial J_P/\partial x + q\partial g(x,t)/\partial t = -qg(x,t)/\tau_P \quad (4b)$$

where J_P is the current density, q is the ionic charge, D_P is the diffusion constant, μ_P is the mobility, τ_P is the recombination lifetime, ε is the constant electric field, and $g(x,t)$ is the Green function in the time-domain. We are interested in finding an expression for $G(x,s\mid x_o)$ defined in the previous section, which is the Laplace transform of $g(x,t)$. Substitution of Eqs. (4a) in Eq. (4b) gives,

$$D_P\frac{\partial^2 g(x,t)}{\partial x^2} - \mu_P\varepsilon\frac{\partial g(x,t)}{\partial x} - \frac{g(x,t)}{\tau_P} = \frac{\partial g(x,t)}{\partial t} \quad (5)$$

RESEARCH ARTICLE

We now introduce the transformation, $g(x,t) = g'(x,t)\exp[-t/\tau_P]$, that helps us to rewrite Eq. (5) as:

$$D_P\frac{\partial^2 g'(x,t)}{\partial x^2} - \mu_P\varepsilon\frac{\partial g'(x,t)}{\partial x} = \frac{\partial g'(x,t)}{\partial t} \tag{6}$$

As shown in Appendix B, the two solutions of Eq. (6) are:

$$G(x,s\mid x<x_o) = \frac{p_O\sinh\sqrt{s/D_P}(L-x)+Q_O\sqrt{s/D_P}\sinh\sqrt{s/D_P}(L-x_O)\sinh\sqrt{s/D_P}x}{s\cdot\sinh\sqrt{s/D_P}L} \tag{7a}$$

$$G(x,s\mid x>x_o) = \frac{p_O\sinh\sqrt{s/D_P}(L-x)+Q_O\sqrt{s/D_P}\sinh\sqrt{s/D_P}x_O\sinh\sqrt{s/D_P}(L-x)}{s\cdot\sinh\sqrt{s/D_P}L} \tag{7b}$$

where $G(x,s\mid x<x_o)$ and $G(x,s\mid x>x_o)$ together represent $G(x,s\mid x_o)$ which is the Laplace transform of $g(x,t)$, p_O is the bulk concentration of the source reservoir, and Q_O is the amplitude of the initial pulse. It is worth mentioning that in Eqs. (7a) and (7b), the effect of mobility and electric field are not directly obvious because of a (x',t') space-time transformation made during the derivation (see Appendix B). However, after Laplace inversion, we can revert to the original $t(x,t)$ space-time domain where the terms containing mobility and electric field are obvious. The inverse Laplace transform of Eq. (7) gives the Green function solutions in the time domain without (Eq. (8a)) and with (Eq. (8b)) the effect of the electric field as follows:

$$g'(x',t') = p_O\left[1-\frac{x'}{L}-\frac{2}{\pi}\sum_{n=1}^{\infty}\frac{e^{-\beta^2 D_P t'}}{n}\sin(\beta x')\right] + \frac{2Q_O}{\pi L}\sum_{n=1}^{\infty}\frac{e^{-\beta^2 D_P t'}}{n}\sin(\beta x')\sin(\beta x_O) \tag{8a}$$

where $\beta = n\pi/L$. Substituting back the initial transformations from (x',t') to (x,t),

$$g(x,t) = p_O e^{-t/\tau_P}\left[1-\frac{x-\mu_P\varepsilon t}{L} - \frac{2}{\pi}\sum_{n=1}^{\infty}\frac{e^{-\beta^2 D_P t}}{n}\sin(\beta(x-\mu_P\varepsilon t))\right] + \frac{2Q_O e^{-t/\tau_P}}{\pi L}\sum_{n=1}^{\infty}\frac{e^{-\beta^2 D_P t}}{n}\sin(\beta(x-\mu_P\varepsilon t))\times\sin(\beta x_O) \tag{8a}$$

In Figure 2, we plot the time variation of the Green function solution $g'(x',t')$ from Eq. 8(a). The channel length is assumed to be 40 Å and the initial pulse, $\delta(x-x_O)$, is applied in the middle of the channel ($x_O = 20$ Å). As shown in the figure, the Green function spreads uniformly

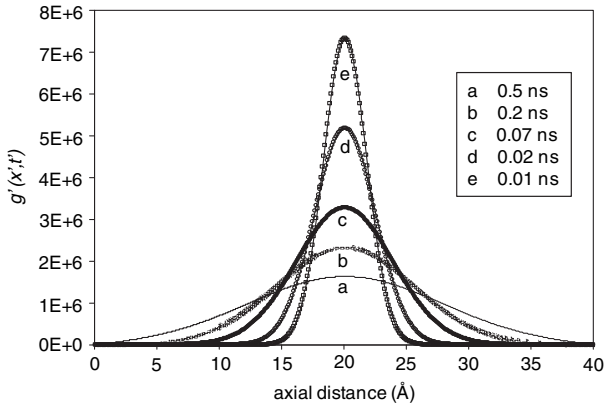

Fig. 2. The figure shows the diffusion-influenced time variation of the Green function from Eq. (8a). The channel was assumed to be 40 Å long and the initial pulse is applied in the middle of the channel. The electric field is not applied here and the pulse decays with time as a result of diffusion.

to either side of x_O, gradually diminishing in peak value due to diffusion. In Figure 3, we plot the same time variation of the Green function solution $g(x,t)$ from Eq. (8b). The channel is 40 Å long and the initial pulse is applied in the middle of the channel. In this case, we notice that the Green function slowly migrates to the right end of the channel caused by the right-side directed electric field and spreads out due to diffusion.

To show the effect of electric field and surface sites on ion transport, we simulated a cylindrical channel (40 Å long and 6 Å wide) using a SILVACO simulation software. In this solid-state simulation tool, silicon is used to mimic the conducting water continuum and silicon oxide to mimic the non-conducting protein walls. The simulation parameters (carrier concentration, ionization degree, and diffusion coefficients) are adjusted in each conducting region to emulate the realistic motion of potassium ions

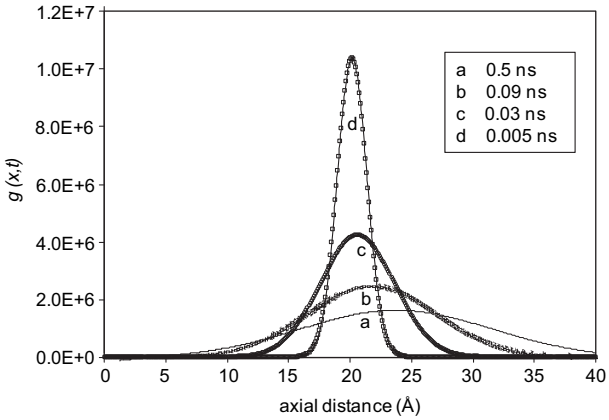

Fig. 3. The figure shows the time diffusion and electric field-influenced variation of the Green function from Eq. (8b). The channel was assumed to be 40 Å long and the initial pulse is applied in the middle of the channel. The pulse decays with time as a result of diffusion and also propagates to the right due to the applied electric field.

inside the channel.[10] The simulations are performed using the discretized PNP Eqs. (4a) and (4b). Figure 4 shows decreased ion concentration inside the cylindrical channel, as predicted by Brownian dynamics.[10] Figure 5 plots the potential profile in the presence of an electric field and increasing surface charges. As shown in the figure, an energy barrier inside the channel is transformed to a potential well by the inclusion of surface charges, thus increasing the chances of ion permeation. The electric field further lowers the potential well towards the sink, making it easier for ions to traverse the channel region.

4. SPECTRAL DENSITY

We now substitute the Green function $G(x, s \mid x < x_o)$ and $G(x, s \mid x > x_o)$ from the previous section (Eqs. (7a) and (7b)) into Eqs. (3a) and (3b) to obtain the exact p.d.f. of a free ion, $\overline{p}(x, s \mid x_o)$ and that of a bound ion, $\bar{q}(x, s \mid x_o)$. Assuming a perfect sink on either side of the channel ($p_0 = 0$) and a unit impulse as the initial state ($Q_0 = 1$) described in Section 2, the p.d.f. of a free ion $\overline{p}(x, s \mid x_o)$ are given by:

$$\overline{p}_1(x, s \mid x < x_o) = \left((s+k_d)\sqrt{\frac{s}{D_P}}\sinh\left(\sqrt{\frac{s}{D_P}}(-L+x_0)\right) \times \sinh\left(\sqrt{\frac{s}{D_P}}x\right)\right)\Big/\left(s\left[-(s+k_d)\sinh\left(\sqrt{\frac{s}{D_P}}L\right) + k_a\sqrt{\frac{s}{D_P}}\sinh\left(\sqrt{\frac{s}{D_P}}(-L+x_0)\right)\sinh\left(\frac{1}{2}\sqrt{\frac{s}{D_P}}x_0\right)\right]\right) \tag{9a}$$

$$\overline{p_2}(x, s \mid x > x_o) = \left((s+k_d)\sqrt{\frac{s}{D_P}}\sinh\left(\sqrt{\frac{s}{D_P}}(-L+x)\right)\right.$$

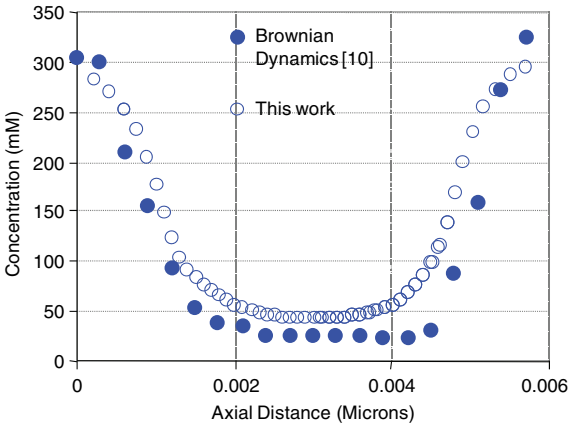

Fig. 4. Comparison of the potassium ion concentration in a cylindrical channel (40 Å long and 6 Å wide) obtained from this model and Brownian dynamics[12] in the absence of electric fields.

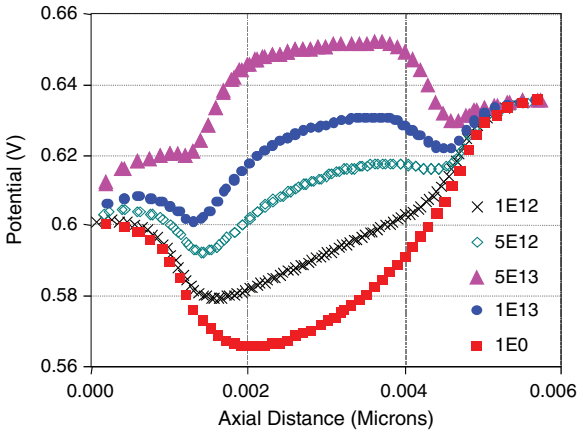

Fig. 5. In the presence of an electric field and increasing surface charge concentrations, the energy barrier is lowered and it is easier for ions to pass through the channel region.

$$\left.\times \sinh\left(\sqrt{\frac{s}{D_P}}x_0\right)\right)\Big/\left(s\left[-(s+k_d)\sinh\left(\sqrt{\frac{s}{D_P}}L\right) + k_a\sqrt{\frac{s}{D_P}}\sinh\left(\sqrt{\frac{s}{D_P}}(-L+x_0)\right)\sinh\left(\frac{1}{2}\sqrt{\frac{s}{D_P}}x_0\right)\right]\right) \tag{9b}$$

The correlation function of interest is the survival probability which is given by,

$$C(t \mid x_o) = \int_0^{x_0} p_1(x, t \mid x_o) + \int_{x_0}^{L} p_2(x, t \mid x_0) \tag{10}$$

The survival probability is an indicationof how successful an ion is to traverse the ion-channel from the source to the sink reservoir (Fig. 1). In other words, survival probability is the probability that a free ion will remain free (or dissociated) and not associate with surface charges on the channel wall. In Laplace domain, it can be expressed as:

$$L\{C(t \mid x_o)\} = \overline{C}(s \mid x_o) = \int_0^{\infty} C(t \mid x_o)e^{-st}dt \tag{11}$$

Using Eqs. (9)–(11), the survival probability is obtained as:

$$\overline{C_1}(s \mid x_o) = \left((s+k_d)\left[-\sinh\left(\sqrt{\frac{s}{D_P}}L\right) + \sinh\left(\sqrt{\frac{s}{D_P}}(-L+x_0)\right) - \sinh\left(\sqrt{\frac{s}{D_P}}x_0\right)\right]\right)\Big/\left(s\left[-(s+k_d)\sinh\left(\sqrt{\frac{s}{D_P}}L\right) + k_a\sqrt{\frac{s}{D_P}}\sinh\left(\sqrt{\frac{s}{D_P}}(-L+x_0)\right)\sinh\left(\frac{1}{2}\sqrt{\frac{s}{D_P}}x_0\right)\right]\right) \tag{12}$$

In a typical electrophysiological experiment, one of the key measured quantities is the power spectral density, $S(f)$, of the ion number fluctuations through the channel. As reported through experimental reports, this noise

induced by ion transport exceeds the background noise by orders of magnitude.[10] As such, the spectral density, $S(f)$, is a valuable source of information about ion movement in a channel's vestibule.[11, 12] Fortunately, we can relate the spectral density to the survival probability as:

$$S(f) = 4Re\{\overline{C}(s = 2\pi fi \mid x_o)\} \quad (13)$$

As shown above, spectral density is the frequency-domain Fourier representation of the correlation function or survival probability in time-domain. For simplicity, let us assume that the initial impulse is given at the middle of the channel ($x_o = L/2$). Using Eqs. (12) and (13), the expression for spectral density is obtained as:

$$S_1(f) = 4.Re\left\{\left(2(2\pi fi + k_d) \times \left[\cosh\left(\frac{1}{2}(\sqrt{2\pi fi/D_P})L\right) - 1\right]\right) \Big/ \left(2\pi fi\left[2(2\pi fi + k_d)\cosh\left(\frac{1}{2}(\sqrt{2\pi fi/D_P})L\right) + k_a(\sqrt{2\pi fi/D_P})\sinh\left(\frac{1}{2}(\sqrt{2\pi fi/D_P})L\right)\right]\right)\right\} \quad (14)$$

To demonstrate some applicability of the above equation and its dependence on the rate constants, we chose a set of rate constants and calculated the spectral density. The channel dimensions are kept same as before. Figure 6 plots the spectral density from Eq. (14) for the case of a fixed $k_a = 10^{-3}$ and values of varying k_d. Figure 7 plots the spectral density of particle number fluctuations obtained from Eq. (14) with fixed $k_d = 10^{-5}$ and varying k_a. At low frequencies ($f < 100$ Hz), the spectral density is flat and then decays with increasing frequency. The frequency roll-off is typically represented as $1/f^{\alpha}$ where the exponent α can be between 1 and 2.[12] In both figures, the bottom curves correspond to the case of free diffusion where the rate constant of association or dissociation is assumed to be infinity. For finite values of the two rate constants, the low-frequency spectral density increases compared to the case of free diffusion. This suggests that free ions associate and dissociate with the binding sites with a finite rate, which increases the fluctuations in ion number and the spectral density. A comparison of both the figures shows that the roll-off slope is more sensitive to the value of dissociation rate constant k_d than that of the association rate constant k_a.

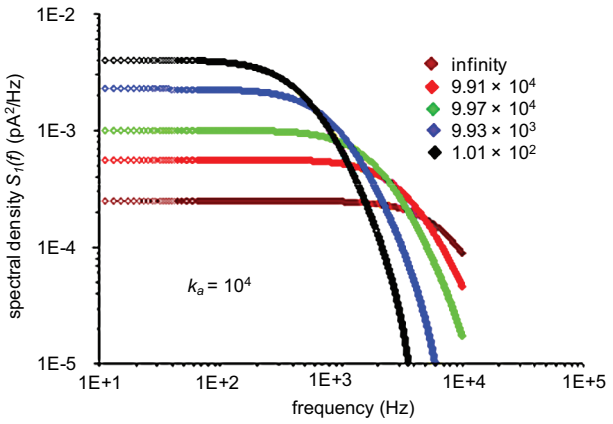

Fig. 6. The spectral density of particle number fluctuations obtained from Eq. (14) with fixed $k_a = 10^4$ and values of k_d varying from bottom to top: infinity (free diffusion), 9.91×10^4, 9.97×10^4, 9.93×10^3 and 1.01×10^2.

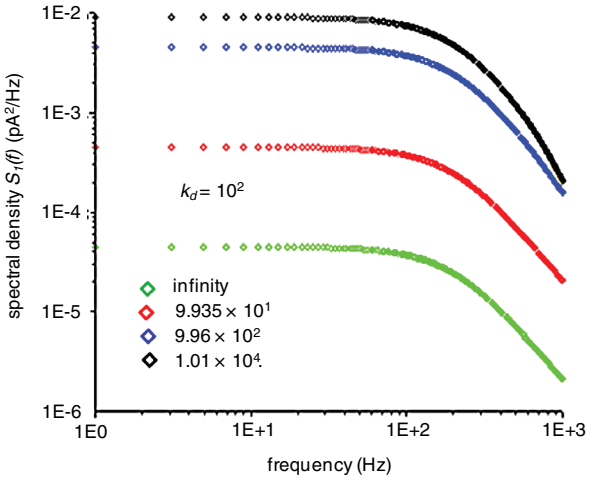

Fig. 7. The spectral density of particle number fluctuations obtained from Eq. (14) with fixed $k_d = 10^2$ and values of k_a varying from bottom to top: infinity (free diffusion), 9.935×10^1, 9.96×10^2 and 1.01^4.

As mentioned earlier, the spectral density can be experimentally determined while other parameters such as survival probability and p.d.f.s are difficult to determine directly from experiments. It is also not possible to determine the rates of association (k_a) and dissociation (k_d) directly from experiments. However, it is possible to extract the above-mentioned parameters by fitting the presented model with experimental data on current noise-generated spectral density of ion channels.[12] The values of rate constants are chosen here to keep the noise magnitude (0.01 to 10×10^{-27} A^2/Hz) and frequency range (10 Hz to 10 kHz) roughlyclose to those observed in actual ion channel experiments.[12] It is worth mentioning that the magnitude of this measured noise is at least 100-fold higher than shot noise or Johnson noise of the channel. Eq. (14) represents the general expression for plotting the spectral density which may be tailored to a different set of rate parameters or channel dimensions depending on the appropriate ion channel under study.

5. DISCUSSION

Here, the modeling of the ion flux is inspired by the geminate excited-state reversible dissociation reaction that requires introduction of Green functions for depicting the transition probabilities of an ion's association or

RESEARCH ARTICLE

dissociation.[8] Theso-called trapping problem, where a molecule diffuses among many static traps, has been studied in the areas of chemical kinetics and material physics.[8] These studies, however, have been limited to solution-phase chemistry (where there are reversible diffusion-influenced reactions in the excited electronic state) or semiconductor physics (where various devices employ the electronic trapping/excitation for their working).[13] In our models, we have extended the application of such diffusion-influenced reversible trapping problems to describe the ionic transport through ion channels and obtain the spectral density of ion number fluctuations.

There are some limitationsinthe derived analytical model. In practical, diffusion coefficient used in our models might not be a constant (in fact, they are time-varying). This is because the restricted diffusion of molecules in biological systems is affected by the presence of different types of barriers/obstacles. This tends to the slowdown of diffusion at long times as compared to barrier-free diffusion.[14] In addition, our calculations assumea single ion channel is in the open state. Realistically, there may be multiple ion channels that may open and close for random time intervals. A single channel may undergo transitions between open, closed, and inactivated states. This channel flickering may contribute to increased spectral density with several corner frequencies which may, however, be challenging to incorporate in the present model.

With new analytical methods being developed and increased computational capability, simulation models of ion permeation are becoming increasing sophisticated andtypically fall into three categories: brownian dynamics, molecular dynamics, and continuum electrostatics.[15, 16] Exact molecular dynamic solution of ion transport in a channel structure is ideally possible but is virtually impossible with today's computational power. For example, to simulate 1 ps of real time for an ion channel model having 1020 amino acid residues, 13,000 water molecules, and 27 sodium atoms would require two hours of computation time.

To reduce the computer time, continuum approximation is selectively applied in these simulations to relatethe ion permeation characteristics to the physical channel structure.[16, 17] With recent explosion in the amount of available genomic and structural data about membrane proteins, computationally efficient approaches arebeing investigated to facilitate a greater understanding of channel properties and functioning.[17] New computational approaches such as semi-Markov chain model[19] and six-state kinetic model[20] have been proposed to predict ion permeation with less computational complexity and comparable accuracy to Brownian dynamics. Recently, synthetic nanopores have been used as experimental test-beds to validate several theories on ion channel transport such as preferential ion selectivity.[21] In this respect, analytical models of ion transport could help complement available simulation models and predict a number of key parameters. This work is an attempt to model the noise fluctuations during electrostatics-based ion transport in a channel environment and relate it to an experimentally measured parameter such as the spectral density. Future work is needed to incorporate the effects of ion selectivity, ion–ion interactions,hydration energy, and multichannel activity in such analytical models with regards to electrophysiological data.[22]

6. CONCLUSIONS

We presented an analytical method for calculating key parameters of ion transport through ion channels including survival probability of a free ion and spectral density of ion number fluctuations. Besides diffusion, the model includes the effects of electric field and reversible binding of free ions with the protein surface charges. The Green function is used to calculate the exact probability density functions of a free or bound ion within the channel's vestibule. The general expression for spectral density shows the interplay of several key parameters governing ion transport, namely rates of association/dissociation, channel dimensions, ion mobility, and frequency. We saw that the spectral density has a 1/f slope and increases with finite rates of association/dissociation between the ions and surface charges.

Appendix A

General Derivation of the p.d.f in terms of the Green Function

Without a loss of generality, we can assume an initial state of free ions at a distance x_o:[9]

$$p(x,0)=\delta(x-x_o),\quad q(x,0)=0 \tag{A1}$$

In Laplace domain, equations 1a and 1b can be written as:

$$(s-£)\overline{p}(x,s\mid x_o)-\delta(x-x_o) = [-k_a\overline{p}(a,s\mid x_o)+k_d\overline{q}(a,s\mid x_o)]\delta(x-a) \tag{A2a}$$

$$s\bar{q}(x,s\mid x_o) = [-k_d\overline{q}(a,s\mid x_o)+k_a\overline{p}(a,s\mid x_o)]\delta(x-a) \tag{A2b}$$

where $\overline{p}(x,s\mid x_o)$ and $\bar{q}(x,s\mid x_o)$ denote the Laplace transforms of $p(x,t)$ and $q(x,t)$, respectively with an initial condition given by Eq. (A1). We introduce the Green function satisfying the equation:

$$(s-£)G(x,s\mid x_o)=\delta(x-a) \tag{A3}$$

Then, in terms of the Green function, Eq. (A2a) becomes:

$$\overline{p}(x,s\mid x_o)=[-k_a\overline{p}(a,s\mid x_o)+k_d\overline{q}(a,s\mid x_o)] \times G(x,s\mid a)+G(x,s\mid r_o) \tag{A4}$$

RESEARCH ARTICLE

From Eqs. (A2b) and (A4), we arrive at the following identities:

$$\overline{p}(a,s\mid x_o)=\frac{G(a,s\mid x_o)}{1+(sk_a/(s+k_d))G(a,s\mid a)}\bar{q}(a,s\mid x_o)$$
$$=\left[\frac{k_a}{s+k_d}\right]\overline{p}(a,s\mid x_o) \quad \text{(A5a)}$$

$$-k_a\overline{p}(a,s\mid x_o)+k_d\overline{q}(a,s\mid x_o)$$
$$=\frac{G(a,s\mid x_o)}{1+(sk_a/(s+k_d))G(a,s\mid a)}\times\left(-\frac{sk_a}{s+k_d}\right) \quad \text{(A5b)}$$

Using Eq. (A5b), the two probability density functions are given by Eqs. (3a) and (3b).

Appendix B

Derivation of the Green Function

Rewriting Eq. (6):

$$D_P\frac{\partial^2 g'(x,t)}{\partial x^2}-\mu_P\varepsilon\frac{\partial g'(x,t)}{\partial x}=\frac{\partial g'(x,t)}{\partial t} \quad \text{(B1)}$$

We use a transformation $x'=x-\mu_P\varepsilon t$ and $t'=t$ on Eq. (B1) yielding:

$$D_P\frac{\partial^2 g'(x',t')}{\partial x'^2}=\frac{\partial g'(x',t')}{\partial t'} \quad \text{(B2)}$$

Using the Laplace transform on Eq. (B2) as:

$$L\{g'(x',t')\}=\bar{g}'(x',s)=\int_0^\infty g'(x',t')\exp(-st')dt' \quad \text{(B3)}$$

with the initial condition $g'(x',0)=Q_O\delta(x'-x_O)$ gives:

$$\frac{\partial^2\bar{g}'(x',s)}{\partial x'^2}-\frac{s}{D_P}\bar{g}'(x',s)=-\frac{Q_O}{D_P}\delta(x'-x_O) \quad \text{(B4)}$$

The above initial impulse $Q_O\delta(x-x_O)$ has amplitude of Q_O at an axial distance $x=x_o$ along the channel. Because of this generalized definition, one can vary the amplitude and location of the initial impulse according to specific needs. The following are the boundary conditions:

$$\bar{g}'(x'=x_O,s)|_{x'<x_o}=\bar{g}'(x'=x_O,s)|_{x'>x_o}$$
$$\frac{\partial\bar{g}'(x',s)}{\partial x'}\Big|_{x_O^+}-\frac{\partial\bar{g}'(x',s)}{\partial x'}\Big|_{x_O^-}=-\frac{Q_O}{D_P}$$
$$\bar{g}'(x',s)|_{x'=L}=0 \quad \bar{g}'(x',s)|_{x'=0}=p_O/s \quad \text{(B5)}$$

It was assumed that the source reservoir has an ionic-concentration p_O, the sink reservoir is perfect, and continuity is maintained before and after the site of initial impulse $x=x_o$. We can now solve Eq. (B4) and obtain the Green function $G(x,s\mid x_o)$ given by Eqs. (7a) and (7b).

Acknowledgments: The work is supported by National Science Foundation (CMMI-1000808).

References and Notes

1. J. Aqvist and V. Luzhkov, *Nature* 404, 881 (**2000**).
2. M. Stevens, *J. Chem. Phys.* 121, 11942 (**2004**).
3. P. C. Jordan, *Biophys. J.* 41, 189 (**1983**).
4. B. Eisenberg, *Biophys. Chem.* 100, 507 (**2003**).
5. E. Frehland, Stochastic Transport Processes in Discrete Biological Systems, Springer, New York (**1982**).
6. W. Nadler and D. L. Stein, *J. Chem. Phys.* 104, 1918 (**1996**).
7. N. Agmon, *J. Chem. Phys.* 110, 2175 (**1999**).
8. H. Kim and K. J.Shin, *J. Chem. Phys.* 112, 8312 (**2000**).
9. N. Agmon, *J. Chem. Phys.* 81, 2811 (**1984**).
10. B. Corry, S. Kuyucak, and S. Chung, *Biophys. J.* 84, 3594 (**2003**).
11. R. S. Eisenberg, M. M. Klosek, and Z. Schuss, *J. Chem. Phys.* 102, 1767 (**1995**).
12. J. Kasianowicz and S. Bezrukov, *Biophys. J.* 69, 94 (**1995**).
13. V. Gopich, K. M. Solntsev, and N. Agmon, *J. Chem. Phys.* 110, 2164 (**1999**).
14. O. K. Dudko, A. M. Berezhkovskii, and G. H. Weiss, *J. Chem. Phys.* 121, 11283 (**2004**).
15. S. Kuyucak, O. Anderson, and S. Chung, *Rep. Prog. Phys.* 64, 1427 (**2001**).
16. D. Gillespie and R. S. Eisenberg, *Eur. Biophys. J.* 31, 454 (**2002**).
17. S. Nekolla, C. Anderson, and R. Benz, *Biophys. J.* 66, 1388 (**1994**).
18. Y. Arinaminpathy, E. Khurana, D. Engelman, and M. Gerstein, *Drug Discovery Today* 14, 1130 (**2009**).
19. D. V. Krishnamurthy and K. Luk, *IEEE/ACM Trans. Computational Biology and Bioinfo.* 8, 273 (**2011**).
20. C. Camacho, *PLoS one* 3, e3342 (**2008**).
21. D. Gillespie, D. Boda, Y. He, P. Apel, and Z. Siwy, *Biophys. J.* 95, 609 (**2008**).
22. C. Boiteux, S. Kraszewski, C. Ramseyer, and C. Girrde, *J. Mol. Model.* 13, 699 (**2007**).

Received: 30 November 2010. Accepted: 23 June 2011.